Motion, relaxation dynamics, and diffusion processes in two-dimensional colloidal crystals confined between walls

Dorothea Wilms,[1] Peter Virnau,[1] Ian K. Snook,[2] and Kurt Binder[1]

[1]*Institut für Physik, Johannes Gutenberg Universität Mainz, Staudinger Weg 7, 55099 Mainz, Germany*
[2]*RMIT University, School of Applied Sciences, Melbourne, Victoria 3001, Australia*

The dynamical behavior of single-component two-dimensional colloidal crystals confined in a slit geometry is studied by Langevin dynamics simulation of a simple model. The colloids are modeled as pointlike particles, interacting with the repulsive part of the Lennard-Jones potential, and the fluid molecules in the colloidal suspension are not explicitly considered. Considering a crystalline strip of triangular lattice structure with $n = 30$ rows, the (one-dimensional) walls confining the strip are chosen as two rigidly fixed crystalline rows at each side, commensurate with the lattice structure and, thus, stabilizing long-range order. The case when the spacing between the walls is incommensurate with the ideal triangular lattice is also studied, where (due to a transition in the number of rows, $n \rightarrow n - 1$) the confined crystal is incommensurate with the confining boundaries, and a soliton staircase forms along the walls. It is shown that mean-square displacements (MSDs) of particles as a function of time show an overshoot and then saturate at a horizontal plateau in the commensurate case, the value of the plateau being largest in the center of the strip. Conversely, when solitons are present, MSDs are largest in the rows containing the solitons, and all MSDs do not settle down at well-defined plateaus in the direction parallel to the boundaries, due to the lack of positional long-range order in ideal two-dimensional crystals. The MSDs of the solitons (which can be treated like quasiparticles at very low temperature) have also been studied and their dynamics are found to be about an order of magnitude slower than that of the colloidal particles themselves. Finally, transport of individual colloidal particles by diffusion processes is studied: both standard vacancy-interstitial pair formation and cooperative ring rotation processes are identified. These processes require thermal activation, with activation energies of the order of $10 T_m$ (T_m being the melting temperature of the crystal), while the motions due to long-wavelength phonons decrease only linearly in temperature.

I. INTRODUCTION

Colloidal systems have been extensively studied, as they are a very useful model system not only for statistical physics but also for modeling nanotechnological devices and self-assembly processes. The great advantage of using colloids lies in the fact that they can be produced with tunable interactions, in different shapes and sizes, and that convenient techniques are available to observe their structure and dynamics directly [1–5].

Therefore, colloidal systems have been investigated under various external conditions both by experiment and simulation. Two-dimensional layers of colloids have been created [6–17], they have been confined mechanically or by laser fields [7,13,17–19], and layers of colloids have been sheared whereby soliton-like excitations have been observed, namely moving kinks and antikinks [20]. They have been used as a model system to study phase transitions [8–10,21] and crystal nucleation in two-dimensional colloidal systems [14], and the crack formation in two-dimensional colloidal crystals has been studied [22]. They have been used to model the glass transition [16,23]. Different boundary conditions [24] and the effect of incommensurate walls on colloidal crystals in two dimensions has been investigated by simulations in which soliton formation was observed [25–28].

In a crystal formed from atoms or small molecules, the dominating type of motion of all particles are small scale (somewhat damped) oscillating motions (due to thermally excited phonons); the amplitude of these motions can only be of the order of 10% of the nearest neighbor distance (or less), otherwise the crystal melts ("Lindemann criterion") [29]. In a colloidal crystal where micrometer-sized particles are suspended in a solvent, these lattice vibrations are overdamped by the random collisions with the solvent molecules, but with respect to the static mean-square amplitude of particles, the behavior is still analogous to crystals formed from small particles.

But although colloidal systems under confinement have been extensively studied with various questions in mind, a thorough study of the basic motion of the particles and solitons and of the diffusion processes inside of colloidal crystals is still missing, and with this paper we are attempting to fill this gap. We shall present here simulations of a model system describing a confined one-component colloidal crystal; the static properties of this system have already been analyzed in previous works [25–28]. We describe in our simulations the damping of oscillations of the particles due to solvent by carrying out a Langevin dynamics simulation (rather than microcanonical molecular dynamics), thereby ignoring hydrodynamic backflow effects, of course, but the latter should not be important for colloidal crystals in thermal equilibrium. Both perfect (defect-free) crystals and crystals containing solitons at the confining walls shall be studied.

Another important contribution to the movement within colloidal crystals is diffusion. The well-known theory of diffusion in crystals states that diffusion either takes place via vacancies or—in perfect crystals like the one we are studying here—via the formation of a hole and a corresponding

interstitial particle [30]. In this paper we will show that in our model system diffusion also takes place by cooperative rotations of groups of particles.

Such cooperative rotation diffusion processes are known to play an important role in glassy materials [31]. In two-dimensional layers of crystals, such as surfaces, a variety of different diffusion mechanisms have been described: Most studies concentrate on hopping vacancies as the direct mechanism [32] or at least as the underlying principle mediating surface diffusion [33] and on the diffusion mechanism of so-called adatoms, which are atoms adsorbed on a surface [34–39], and on the questions how thermal vacancies are created and destroyed and what role the surface plays in this process [40].

Cooperative ring rotations of colloidal particles in three-dimensional crystals have been observed and investigated in the context of superheated materials, in which they were part of the melting process [41,42]. But to our knowledge, there are only two studies reporting on cooperative ring rotation processes distinctly below the melting transition: Using temperature-accelerated dynamics (TAD) [43,44], Montalenti *et al.* have found evidence of such mechanisms in a two-dimensional layer of crystalline atoms in a periodic potential [45] and in Cu grain boundaries [46], although they were extremely rare, especially in the latter case. In this paper, we will show, that in our two-dimensional model system cooperative ring rotation phenomena occurred quite frequently and involved different numbers of particles.

In the next section we will describe the model system and simulation parameters. Following it, we will show our results for the motion of the particles in the case without solitons, during the equilibration into the defect structure, and for the case where the transition has taken place. In Sec. IV we will describe the diffusion mechanism which we have observed, and in Sec. V we will summarize our findings.

II. MODEL SYSTEM AND PARAMETERS

We are considering a two-dimensional colloidal crystal with a hexagonal lattice structure. In the x direction we are applying periodic boundary conditions, while the system is confined in the y direction by walls consisting of two rows of frozen particles (Fig. 1). All particles interact via a purely repulsive potential,

$$V(r) = \varepsilon[(\sigma/r)^{12} - (\sigma/r_c)^{12}]\left[\frac{(r - r_c)^4}{h^4 + (r - r_c)^4}\right], \quad (1)$$

with parameters $r_c = 2.5\sigma$ and $h = 0.01\sigma$. This potential does not directly correspond to any experimentally realizable situation, but as there are no experiments available for direct comparison at the moment, we chose the r^{-12} dependence with the cutoff and shift due to the computational efficiency of a strictly short-ranged potential and added a smoothing factor for differentiability. Note that in qualitative respects Eq. (1) can be taken as a generic model for a broad class of colloidal particles with short-range repulsive interactions (due to screened Coulomb interactions or due to polymer brush coating, etc.). Henceforth, we chose units of temperature and length such that $\varepsilon = 1$ and $\sigma = 1$.

The simulations are carried out using Langevin dynamics [47] using the program package HOOMD-BLUE [48,49]. This
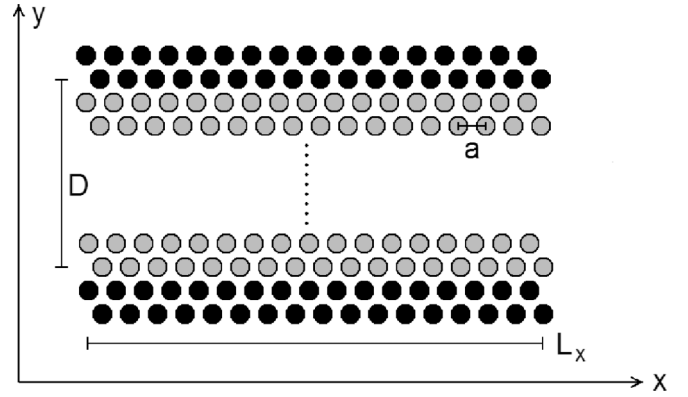

FIG. 1. The system geometry, showing the fixed wall particles (black spheres) and the mobile particles (gray spheres). The orientation of the coordinate axes is indicated, as well as the lattice spacing of the triangular lattice (a) and the linear dimensions L_x, D of the system.

program is designed to run on graphic cards, where, due to the parallelization on the internal processing units, large system sizes can be simulated. Thus, most simulations were carried out using $M = 73\,440$ particles (including walls), i.e., 64 800 mobile particles. However, consumer graphic cards (which we initially used in this study) have substantially more processing power, when single precision accuracy is used, which proved not to be accurate enough for our system at temperatures $T < 1.0$. Therefore, we had to run the simulations at the lower temperatures on conventional CPUs (but still using the program package HOOMD-BLUE, which can also be used on CPUs). As this led to a considerable increase in the computational times, we reduced the system size to $N = 3672$ particles, including walls, i.e., 3240 mobile particles wherever possible when we had to run the simulations on CPUs. These simulations were then carried out on the local computer cluster, with a parallelization on eight cores, where they needed 2–48 h, depending on the simulation.

In the simulations, we apply Langevin dynamics with a velocity-Verlet integration scheme. A force $\vec{F} = -\gamma\vec{v} + \vec{F}_{\text{rand}}$ is added to the force exerted on each particle by the interaction with its neighboring particles [50,51]. Here, γ is a friction coefficient to be specified, $\vec{v}$ is the particle's velocity, and $\vec{F}_{\text{rand}}$ is a random force with a magnitude chosen via the fluctuation-dissipation theorem to be consistent with the specified drag γ and the chosen temperature T. We used a time step of $\Delta t = 0.002$, a friction coefficient of $\gamma = 0.5$ (unless otherwise specified), and a temperature of $T = 1.0$ (unless otherwise specified). Note that our particles have mass $m = 1$ and that the time t is measured in the standard molecular dynamics time unit $\tau = t\sqrt{\frac{\epsilon}{m\sigma^2}}$.

Of course, using a Langevin integrator neglects the hydrodynamic interactions between the particles and between the particles and the confining walls. It also cannot model the different viscosities that occur in a confined system: Close to a wall, the motion of the particles is restricted and the viscosity is, therefore, larger than further away from the walls. This increased friction close to the walls would slow down the dynamics but presumably not change it qualitatively. Including hydrodynamic interactions between the particles might even
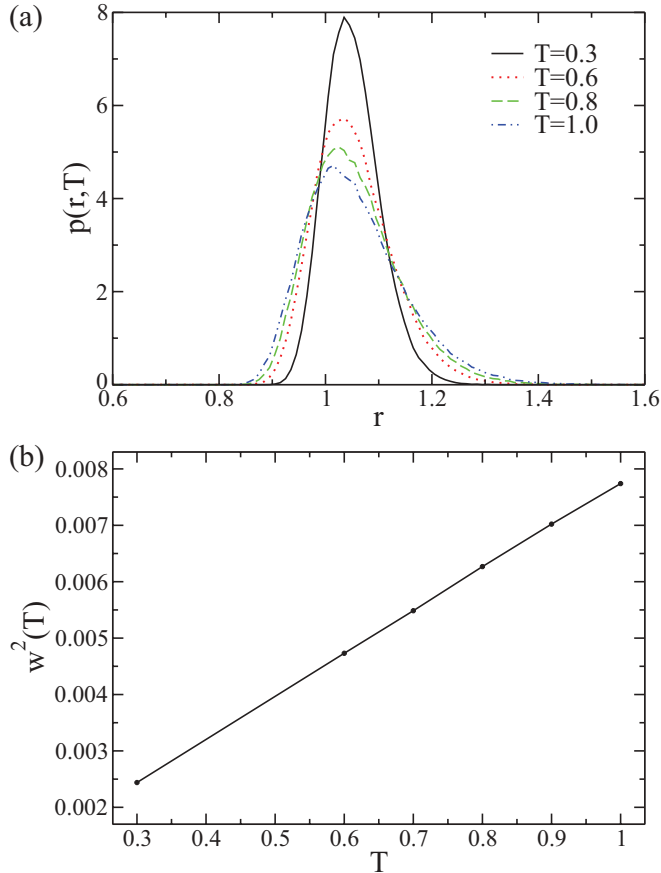
FIG. 3. (Color online) Stress anisotropy $\delta\sigma = \sigma_{xx} - \sigma_{yy}$ curve showing at which values of the misfit Δ the structural transition occurs which reduces the number of rows parallel to the walls. The broken line shows the exact location of this transition in equilibrium, which was obtained using the phase-switch Monte Carlo method [28].

FIG. 2. (Color online) (a) The distribution of the distance r between nearest neighbor particles in the crystal: For each particle, the distance to its six nearest neighbors was used. Different temperatures T as indicated. Distributions are normalized to area = 1. (b) Squared width of the distribution, defined as $w^2(T) = \frac{\langle r^2(T)\rangle - \langle r(T)\rangle^2}{\langle r(T)\rangle^2}$. Simulations in the fully commensurate case with 30 crystalline rows.

enhance the rate at which the cooperative ring diffusion processes occur, which we will describe below. Therefore, our study is a rather qualitative description of the variety of effects present in colloidal crystals.

All simulations were carried out below the melting temperature of $T_m = 1.35$ [52] for our chosen density of $\rho = 1.05$. In Fig. 2 we show the result of computing the fluctuation in the distance between nearest-neighbor particles in the crystal by plotting the distribution of the distances to the six nearest neighbors of each particle versus this distance as a function of the temperature. As expected, this distribution becomes broader for higher temperatures. From this graph one can verify that the relative fluctuations are clearly smaller than what would be expected near melting (from a Lindemann-type criterion). In the commensurate case, the confined crystal has an essentially defect-free triangular crystal structure.

For completeness, we recall now the main facts about the structural transition and associated soliton formation occurring when the crystal is exposed to uniaxial compression: If the walls are placed closer together, then in the commensurate case, a structural transition occurs and the number of rows parallel to the walls is reduced. We define the misfit Δ between
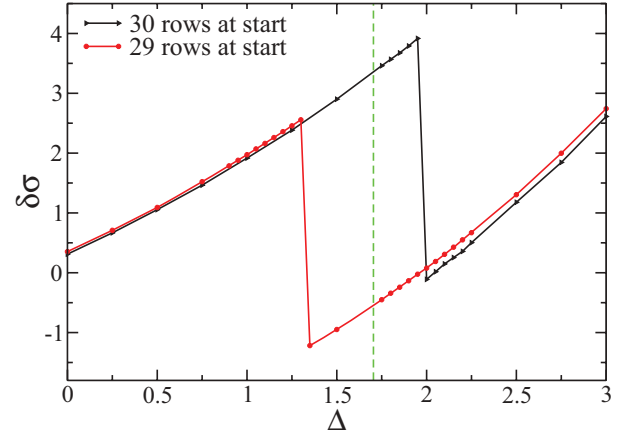
the actual distance D between the two walls and their distance $D_0 = n_y a \sqrt{3}/2$ in the commensurate case as

$$D = (n_y - \Delta)a\sqrt{3}/2, \qquad (2)$$

where a is the lattice constant in the commensurate case (see Fig. 1).

In the present system, we started with 30 rows, which transformed into 29 rows at a misfit of about $\Delta = 2.0$, as can be read off from the stress curves shown in Fig. 3. Note that the components of the stress tensor $\sigma_{\alpha\beta}$ are straightforwardly sampled using the virial formula, as usual. This plot also shows that a system with 29 rows is already metastable at smaller values of the misfit, as simulations starting out with 29 rows showed that the system does only spontaneously rearrange itself into 30 rows until a misfit of about $\Delta = 1.4$. The exact location of the transition without the obscuring hysteresis has been found by applying the phase-switch Monte Carlo method [28].

As the number of particles remained constant in the system at all times, a transition from 30 rows to 29 rows means that the particles which used to be in the 30th row have to be distributed in the rest of the crystal. Earlier work by Chui *et al.* [25–27] has shown that the preferred way of arranging those extra particles is by putting the same number of extra particles in each row except the rows directly adjacent to the walls, which remain free of extra particles due to the stabilizing effect of the walls. Thus, an energetically elevated situation is created where (in the specific case of a system with 3240 mobile particles) $n_{\text{inner rows}} = 112$ particles have to be placed into the $n_{\text{adjacent to walls}} = 108$ minima of the potential created by the 108 particles sitting in the row directly adjacent to the walls. This is illustrated in Fig. 4(a). It is energetically favorable for the system to restrict the mismatch in its rows to small areas of the crystal, thus creating "solitons," which are areas where the lattice structure is locally disturbed. This is shown in Fig. 4(b).
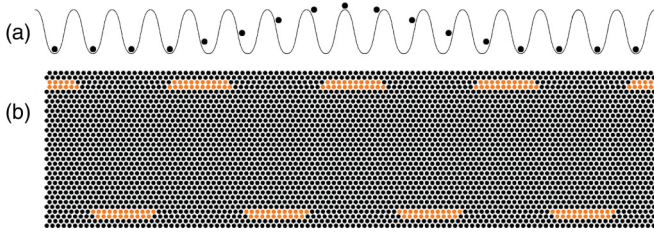
FIG. 4. (Color online) (a) Putting $n + 1$ particles in a periodic potential with n minima creates a soliton configuration, i.e., over a range of several lattice spacings particles are displaced from the potential minima (schematic). (b) Soliton configuration in a lattice of $N = 3672$ particles (including walls) when the particles are arranged into 29 rows. Particles which are part of the solitons are marked in orange (light gray). "Ideal" configuration for $T = 0$ is shown.

In the following, we will refer to the rows directly adjacent to the walls as row 1 and row 30, respectively, and to the inner rows as row 2–29.

In the following section, we shall focus on the mean-square displacements of the particles as function of time, with the motivation being that this type of information, in principle, is also experimentally accessible via particle tracking techniques.

We will use two different definitions of the mean-square displacement (MSD) of the particles: By "MSD with respect to the starting configuration" (M_s) we refer to the definition $M_s(t) = \langle (x(t) - x(0))^2 \rangle_N$, where $\langle \cdots \rangle_N$ denotes the average taken over all (mobile) particles in the system, while "MSD with respect to the time difference between the configurations" (M_t) refers to the definition $M_t(\Delta t) = \langle (x(t) - x(t + \Delta t))^2 \rangle_{N,t}$, where now $\langle \cdots \rangle_{N,t}$ denotes the average taken over all (mobile) particles in the system *and* over all configurations which are a time interval Δt apart from each other.

III. RESULTS ON THE RELAXATION OF PARTICLES AND SOLITONS IN COLLOIDAL CRYSTALS

A. Localized motions of particles confined in "cages" formed by their neighbors

When the system starts out with 30 crystalline rows, $N = 64\,800$ mobile particles, and without misfit, we obtain the MSD with respect to the time difference (M_t) for the particles in x and y direction shown in Fig. 5. Here, like in all graphs of this kind (unless otherwise stated), we printed out configurations after every 50 steps and averaged over 500 configurations. In the following we define one MD time unit by multiplying the number of integration steps with the time step $\Delta t = 0.002$. So one MD time unit corresponds to 500 integration steps.

The starting configurations were equilibrated for 2×10^6 steps before the simulation runs were started. One can see an overshoot at small time scales. This is expected in a crystal as it is due to the repelling forces which the particles experience when they are displaced from their ideal lattice position and, thus, come closer to their neighboring particles. These forces act similarly to a harmonic potential, pinning particles to their lattice sites, therefore they cause this oscillatory behavior in the MSD. But as the oscillation is strongly damped and modified by random kicks, only this overshoot is clearly visible. At slightly larger time scales, the MSD reaches a plateau. This
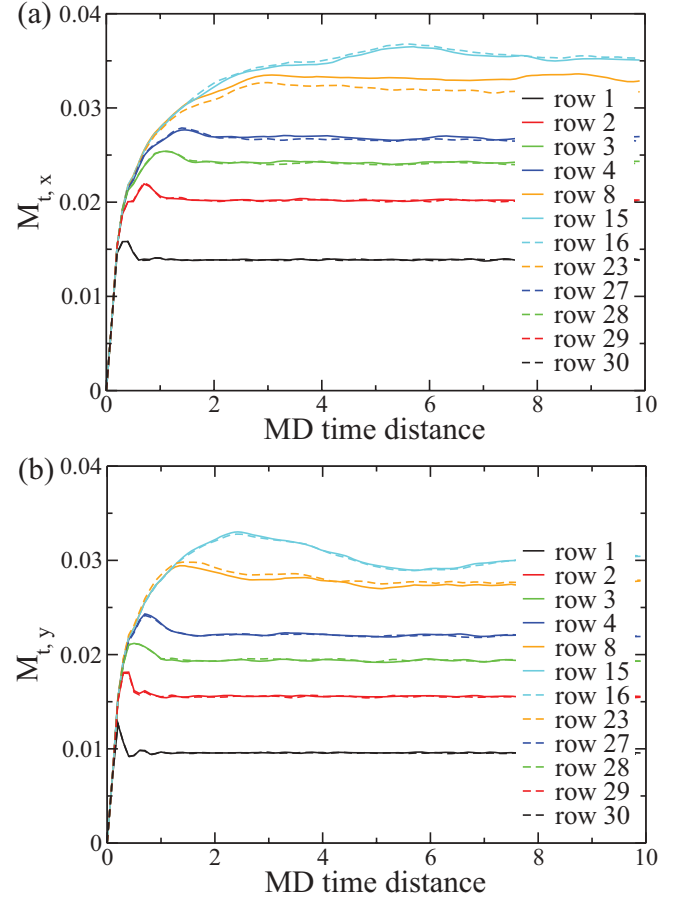

FIG. 5. (Color online) MSD with respect to the time difference (M_t) in x (a) and y directions (b) for a system with 30 rows without misfit. Due to the symmetry of the system, rows 1 and 30, 2 and 29 etc. should on average yield the same curves. Temperature $T = 1.0$. Each MD time unit corresponds to a difference of 500 integration steps as the time step was $\Delta t = 0.002$.

plateau is also expected, because the structured walls are pinning the crystal (as a whole) to its position and do not allow any center-of-mass movement. Thus, the particles are localized near their equilibrium sites. One can also see that in y direction the values are of the same order of magnitude as the crystal is not compressed. They do differ slightly, however, as it makes a difference whether there are fixed wall particles or periodic boundary conditions, of course.

If one studies the same MSDs at a misfit of $\Delta = 1.5$, where the transition to 29 rows has not taken place yet, the values are smaller as the system is compressed and less space is available to the particles (Fig. 6). Apart from this, the proximity of the transition does not show up in the MSDs.

Note that the time-dependent mean-square displacements show in the inner rows (e.g., row 8 and 23, or 15 and 16, respectively) some flat maximum at time ≈ 2. While rows 15 and 16 are adjacent to each other, and, hence, motions of particles in these rows are strongly correlated to each other, rows 8 and 23 are rather remote from each other (they are only equivalent due to the symmetry of the system, since both corrugated walls are equivalent). Hence, this particular feature of the MSD is not a consequence of insufficient averaging but a
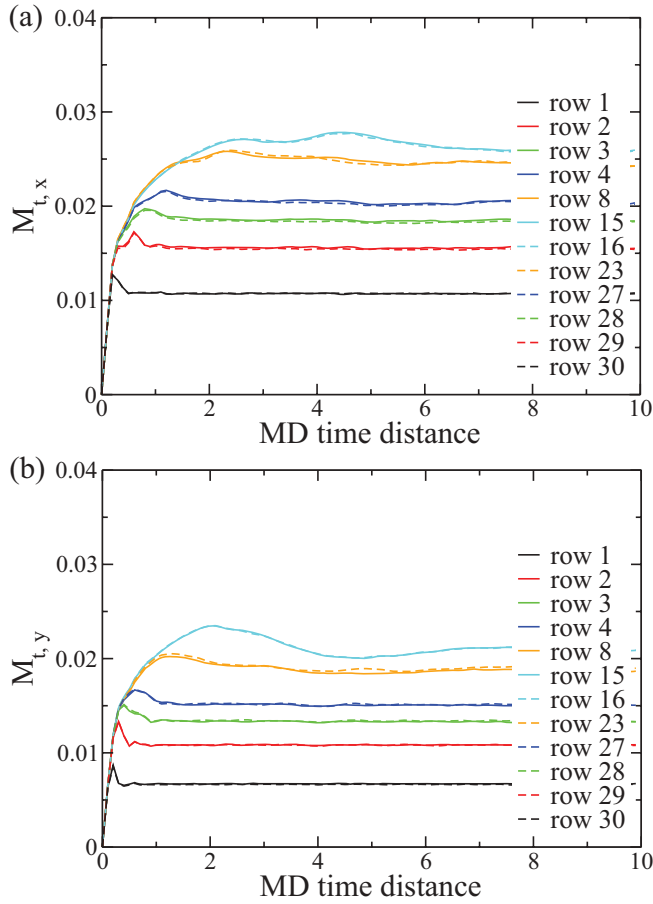
(a)

(b)

FIG. 6. (Color online) As described in the caption to Fig. 5 but for a system with 30 rows at a misfit of $\Delta = 1.5$, where the transition to 29 rows has not taken place yet.

real effect. It also is easily understandable that the mean-square displacements are larger in the center of the slit: Due to the corrugated walls, all phonon-type excitations are constrained to have zero amplitude at the boundaries. A phonon with wavelength $\lambda/2 = D$ then has its maximum amplitude at $y = D/2$.

Figure 7 shows the M_t for an uncompressed bulk system for comparison. As expected, the averaged MSDs are larger when no walls are present. Furthermore, they do not exhibit a real plateau as the center of mass is not fixed without structured walls. Additionally, this figure shows the influence of finite-size effects in connection with the shape of the system in the case where no walls are present: The "square system" behaves like a real bulk crystal where the particles are pinned to their lattice site rather strongly, while in the elongated system only the MSD in the x direction shows this behavior. As the number of rows is significantly smaller than the number of particles per row here, it is energetically possible for the rows to bend and assume an almost wavelike configuration, which leads to significantly larger values of the MSD in the y direction. But, of course, this effect does not occur when walls stabilize the rows.

B. Slow dynamics due to soliton formation

If one starts out with 29 rows at a misfit of $\Delta = 2.2$ or, alternatively, waits long enough until the configuration which
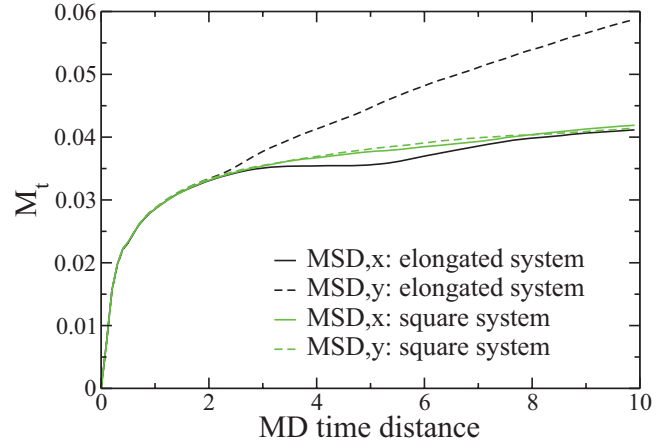

FIG. 7. (Color online) MSD with respect to the time difference (M_t) in x and y directions for a system with 240×270 particles ("square system") and for an elongated system with 2160×30 particles without misfit. Temperature $T = 1.0$. Each MD time unit corresponds to a difference of 500 integration steps as the time step was $\Delta t = 0.002$.

started out with 30 rows at this misfit has fully equilibrated and a regular soliton pattern has evolved, one obtains the values for the M_t as shown in Fig. 8.

One can see from Fig. 8 that the MSD has not reached a plateau, even at an MD-time difference of 30 (=1500 integration steps), for the inner rows, which means that there is some diffusion, which clearly does not involve the rows directly adjacent to the walls. This is not suprising as the rows directly adjacent to the walls retain their original number of particles and are, therefore, still commensurate to the walls and pinned to their position by them, whereas the inner rows have a different number of particles now as one row has disappeared and the particles from this row have been distributed among the inner rows. Therefore, they are no no longer commensurate with the structure of the walls and, thus, can make a translational movement along the walls as the potentials created by the wall particles can no longer hold them in their original positions. In fact, for
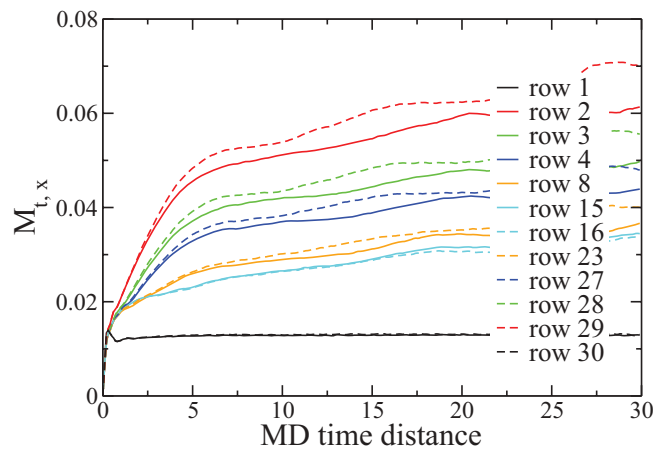

FIG. 8. (Color online) M_t in the x direction for a system which started with 29 rows and was equilibrated at a misfit of $\Delta = 2.2$ (where 29 rows are stable). Temperature $T = 1.0$.

infinite two-dimensional crystals it is well known that the static mean-square displacement of a particle relative to its reference position in the ideal perfectly rigid crystal lattice diverges as the center of mass drifts. In the x direction parallel to the walls we, hence, expect for the rows 2, . . . ,29, which are no longer pinned by the walls that MSD($\Delta t \to \infty$) $\to \infty$, unlike the commensurate case of Figs. 5 and 6, where the whole crystal is pinned by the boundaries, and for any finite slit thickness D we have a finite value of the MSD($\Delta t \to \infty$) for all rows.

One can also see that, generally, the diffusion in row 2 and row 29 has the largest values, while the MSD is smaller again for rows further inside the crystal and has a minimum value for the rows directly next to the walls. This differs fundamentally from the situation shown in Fig. 5 and 6, where row 1 and row 30 also had the smallest values of the MSD, but the MSD grew larger with increasing distance from the walls instead of displaying a maximum in the rows 2 and 29 and becoming smaller again inside of the crystal. This can be explained by the influence of the solitons (in the simulations with 29 rows) which cause considerable movement in the crystal. As we will show in the following section, these solitons are present in the rows next to the rows directly at the walls, i.e., they are sitting close to the walls, thus creating the maximum of the MSD in row 2. They also cause a certain amount of disorder and movement in the rows next to them; therefore, the MSD now decreases towards the inner part of the crystal, while the MSD used to increase due to the decreasing influence of the stabilizing walls in the case without solitons. The rows directly adjacent to the walls were stabilized by the walls in both cases and, thus, always showed the smallest values of the MSD.

When the walls are placed closer together, creating a misfit of $\Delta = 2.2$, it takes some time until all solitons are created in this very large system. While this happens, one can watch the "MSD with respect to the time difference" grow. This is especially visible for those rows in which the solitons are created, i.e., row numbers 2, 3, and 4. The effect is visible both in the x direction and the y direction of the MSD, although now one can see differences in the size of the MSD in the x and y directions. Examples of this are shown in Fig. 9.

While in the commensurate case characteristic times needed to equilibrate the system are of the order of a few MD time units, Fig. 9 reveals that the time needed to equilibrate MSD (Δt) in the incommensurate case is of the order of about 2000 MD time units (for the large system comprised of 64 800 mobile particles; for smaller systems it is quicker). These large times are understandable, since the formation of the soliton staircase pattern requires the nucleation of defects moving from one boundary to the opposite boundary, as described in detail by Chui *et al.* [26] in the framework of Monte Carlo simulations.

Figure 9 also shows that the amplitudes of the curves obtained for row 3 are larger than the ones for row 2. The curves for row 4 (not shown here) are qualitatively very similar, only with an even larger amplitude than the ones for row 3. The fact that the amplitudes of the particles in the inner rows (for example, in row 3) remain slightly larger than those in row 2 indicates that if the system is equilibrated from a 30-row-structure into a 29-row-structure and the solitons are formed at random positions, there is more disorder in the inner rows (which is typical for the case of 30 rows, compare
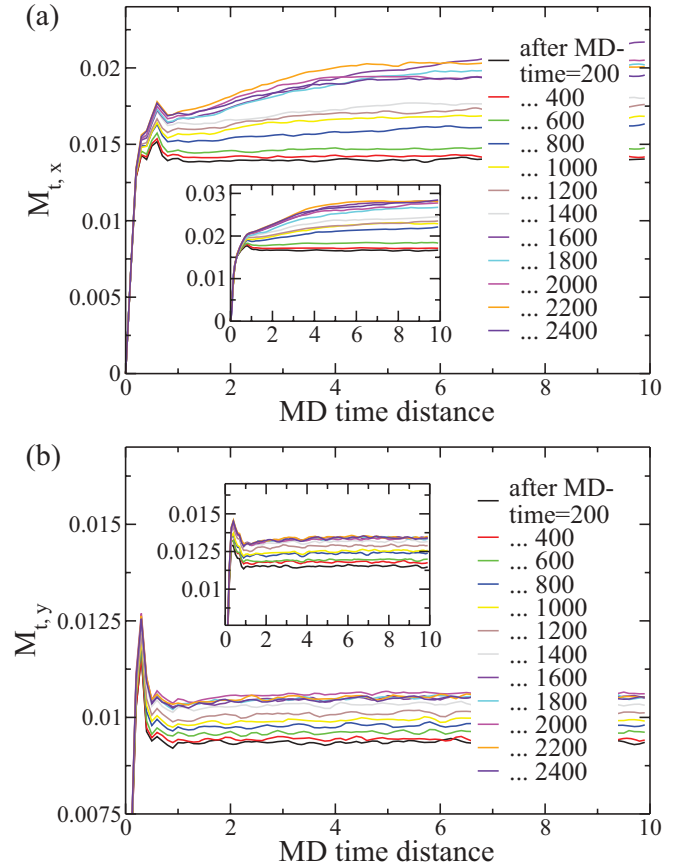

FIG. 9. (Color online) Change of the M_t in the x direction (a) and y direction (b) as solitons are created. Large graphs show curves for row 2, insets for row 3. System started out with 30 rows at a misfit of $\Delta = 2.2$ and slowly solitons were created and the structure changed into 29 rows. Temperature $T = 1.0$.

Figs. 5 and 6), while if the system starts off with 29 rows and a corresponding "perfect" soliton pattern, there is more movement in the rows closer to the walls (see Fig. 8). This behavior can, in principle, change on very long time scales as the solitons repel each other and thus push each other closer to the walls and into a more regular staircase pattern. But usually the structure forming by equilibrating a 30-row-structure into 29 rows gets stuck in a more disordered state and exhibits a less regular soliton pattern and a slightly higher stress even on long time scales.

One can also study the M_t for different values of the misfit Δ as shown in Fig. 10 for different rows. One can see that for relatively small misfits the structure with 30 rows remains stable (as Chui *et al.* have seen in their hysteresis curves as well), but the MSD of the particles shrinks with increasing misfit since there is less space available for local motion in this compressed crystalline structure. At larger misfits (shown are $\Delta = 2.2$ and $\Delta = 2.5$) the structure has changed to 29 rows and solitons have been created, which changes the shape of the curve of the MSDs in the direction parallel to the walls due to the solitons' mobility. But it is also visible in the MSDs in the direction perpendicular to the walls: Instead of decreasing further due to the decreasing space between the walls, the MSD at $\Delta = 2.2$ is significantly larger than at $\Delta = 1.8$ (prior to the
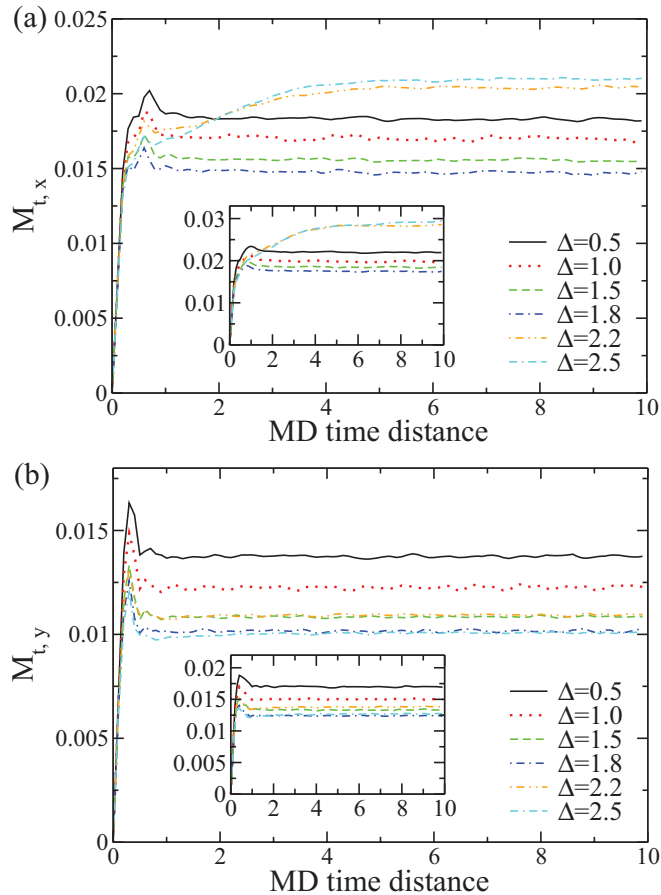
FIG. 10. (Color online) M_t in the x direction (a) and y direction (b) in row 2 of the system (large graphs) and row 3 (insets) for a system starting out with 30 rows at the indicated values of the misfit Δ. Temperature $T = 1.0$.

transition) and instead resemble the values at $\Delta = 1.5$ as the formation of solitons increases the mobility of the particles also in the y direction. Of course, a further increase of the misfit reduces the MSD again, which is demonstrated for the case of $\Delta = 2.5$, where the MSD in y direction is only of the order of that at $\Delta = 1.8$ prior to the transition. Also in Fig. 10 the values of the MSDs are larger for row 3 than for row 2 (and even larger for row 4, but, again, not shown as the curves look qualitatively very similar to the ones displayed for rows 2 and 3) as we used starting configurations consisting of 30 rows at every value of the misfit.

C. Relaxation dynamics of equilibrated soliton structures

If one tries to calculate the M_t of the solitons itself (which was done only in the small system with 3240 mobile particles), one has to be careful to subtract their center-of-mass movement. Even though the particles themselves show a very small (on the time scale we are studying here, almost invisible) center-of-mass movement, the soliton pattern moves around significantly. In this movement, the soliton pattern hardly changes, i.e., the distances between the solitons remain more or less constant, but the pattern as such can easily move along the x direction. Because, after all, solitons are only those areas where some particles are closer to each other than they are on
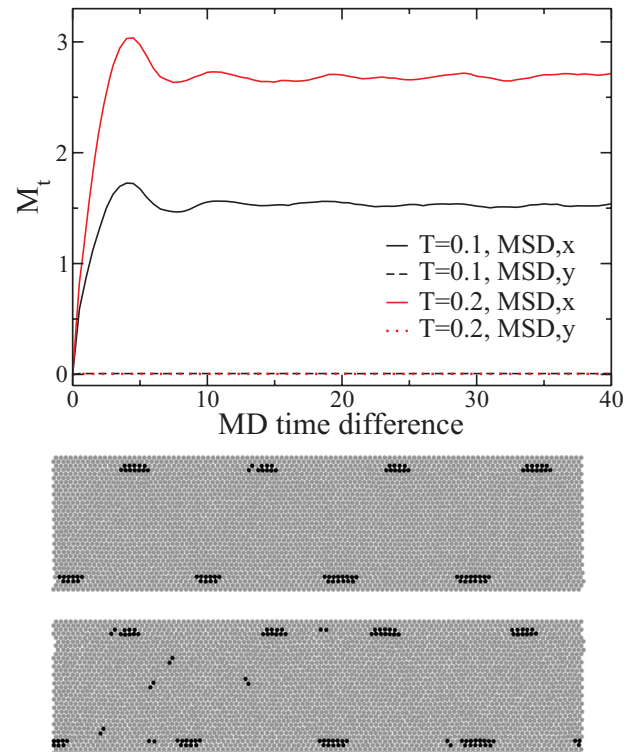

FIG. 11. (Color online) M_t in x and y directions of the solitons at the indicated temperatures for simulations at $\Delta = 2.2$, averaged over the eight solitons that appeared and averaged over 20 runs. Please note that the center-of-mass diffusion of the soliton pattern as a whole has been subtracted from the solitons' movements. This center-of-mass diffusion of the pattern was quite large (of the order of half a distance between solitons). Simulations started with 29 rows and were equilibrated before measuring. System size is $N = 3672$ particles (including walls). Snapshots give examples of which particles are identified as part of solitons (black) in simulations at $\Delta = 2.2$, starting out with 29 rows, at $T = 0.1$ (upper) and at $T = 0.2$ (lower snapshot). For details see text.

average, because some of the extra particles that stem from the row that has disappeared in the $n \rightarrow n-1$ transition in the number of rows now are localized there. So it only takes a few particles to make a small lateral movement and the soliton already changes its position.

When one compares the amplitude of the mean-square displacement of solitons shown in Fig. 11 with that of the individual colloidal particles (Figs. 5 and 6) of the rows close to the immobile walls, several differences are worth mentioning: For individual particles, mean-square displacements in x and y directions are of the same order of magnitude. For solitons, in contrast, mean-square displacements in the y direction are completely negligible, while in the x direction they are an order of magnitude larger than the corresponding value for the colloidal particles. This is the case, because the two rows of solitons (close to the upper and lower walls, respectively) strongly repel each other and, therefore, the solitons remain very close to the walls and almost immobile in the y direction. At the same time, they can easily move in the x direction as they are regions of increased particle density, which already moves if only a few particles make a small coordinated movement in the same direction. While the

soliton staircases are essentially one-dimensional objects, they create a two-dimensional displacement field throughout the whole crystalline strip: This causes the zig-zag type correlation in the arrangement of the solitons near the upper and lower boundaries in Fig. 11. Also the time scale for the oscillatory convergence to the plateau now is of the order of 10 MD steps, while it was of the order of 1 MD step for the particles themselves. This result is expected, recalling the estimates for the small "spring constant" that maintains the average distance between solitons [27]. It also confirms that, in this particular case, Monte Carlo simulations like the ones used by Chui *et al.* in order to determine the potential and spring constant acting between the solitons yield reasonable results for the movements of the particles.

The snapshots shown in the same figure show some representative soliton configurations, where all particles which the code identifies as "possibly being part of a soliton" are marked in black. Of course, only clusters of a certain size of these particles are actually counted as solitons, so the wrongly identified particles somewhere in the middle of the system (especially at slightly higher temperatures) do not disturb the statistics. As it is quite difficult to distinguish particles which do or do not belong to solitons for higher temperatures, only $T = 0.1$ and $T = 0.2$ were used here.

IV. OBSERVATIONS OF DIFFUSION IN SIMULATIONS OF COLLOIDAL CRYSTALS

We now return to uncompressed commensurate crystals ($\Delta = 0$), where at $T = 1.0$ the snapshots reveal in the overwhelming majority of cases a defect-free triangular crystal structure. This is not surprising as it is known that the density of vacancies and interstitials in $d = 2$ for any nonzero temperature is also nonzero in thermal equilibrium [29,53], but very small at temperatures significantly below the melting transition [25,52], which occurs at $T_m = 1.35$ for our system. We ask whether in such almost ideal crystals still some diffusion of particles occurs. In principle, this question is relevant for unconfined crystals (to be simulated using periodic boundary conditions in both the x and y directions) as well, but we focus here on diffusion in a system confined by structured walls as a by-product of our studies in the preceding section. To study this question, we consider a large system comprised of 73 440 particles and long time scales. Also MSDs of the particles need to be investigated over much longer time intervals than the ones we considered before.

If one studies the MSD with respect to the starting configuration (M_s) shown in Fig. 12 (again for $T = 1.0$ and for the larger system), for the case without a misfit, one gets a first idea about diffusion processes inside the crystal: Although the crystal structure is stable, there is a considerable amount of diffusion. This diffusion does not happen continuously, but every now and then larger groups of particles change their position. Although translational invariance is present only in the x direction, the diffusion of particles involves both the x and y coordinates as the particles have to move from one crystalline lattice site to another one. A center-of-mass movement is excluded due to the presence of the structured walls which fix the crystal also in the x direction. And as the values of the MSD are typically quite small in this system
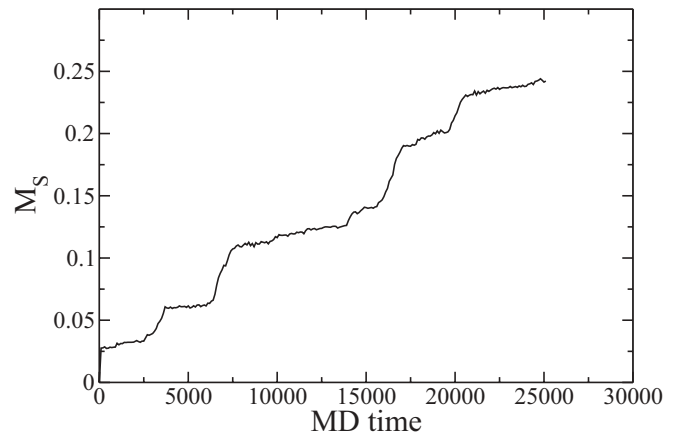

FIG. 12. Example of an MSD with respect to the starting configuration (M_s) for a system with $N = 73\,440$ particles (including walls), $\Delta = 0$ and 30 rows at $T = 1$. In spite of this diffusion, the structure remains crystalline.

(most particles only move by a few lattice spacings, if at all), we will study the MSD as a whole and not specifically its x or y component here (which would mostly differ from each other due to the orientation of the crystalline rows along the x axis). Of course, the size of the MSDs as a whole would probably be larger in the case without walls.

In order to investigate this phenomenon, one can look at snapshots of the system, where all particles which are no longer in their initial lattice position have been marked. A few typical sections of such snapshots are shown in Figs. 13 and 14. Obviously, there are a few circular or ringlike dislocations, where in a group of particles, each particle has jumped onto the lattice site of its neighboring particle, and as the ring is closed, the motion stopped here (Fig. 13). In other parts of the crystal, many particles have left their initial lattice site and have jumped onto some other particle's initial position instead (Fig. 14). The system is still crystalline here and shows a clear hexagonal lattice structure despite the fact that so many particles are no longer in their initial positions as one can see in the lower figure. Also, the disorder present due to phonons (particles being somewhat displaced from their ideal positions in the perfectly rigid structure at temperature $T = 0$ in a coherent, collective way) can be virtually recognized.

The well-known theory of diffusion inside crystals states that diffusion takes place through the creation of a pair of one interstitial particle sitting no longer on the "allowed" lattice sites but moving somewhere in between them and a hole, which it leaves behind and which can diffuse as particles from adjacent lattice sites can jump into it. The formation of such pairs of interstitials and vacancies is induced by thermal fluctuations. This mechanism is prevalent in those areas of the snapshots where many particles have left their initial lattice sites and sit on different lattice sites instead. Naturally, this process involves many particles as the interstitial as well as the hole perform a random walk. At the temperatures we studied here, the density of holes and interstitials is still extremely low, so the interaction of two of such pairs is excluded. Therefore, the diffusion process only stops when this particular pair of vacancy and interstitial happens to be in the same position again and recombine. Despite the fact that they attract each
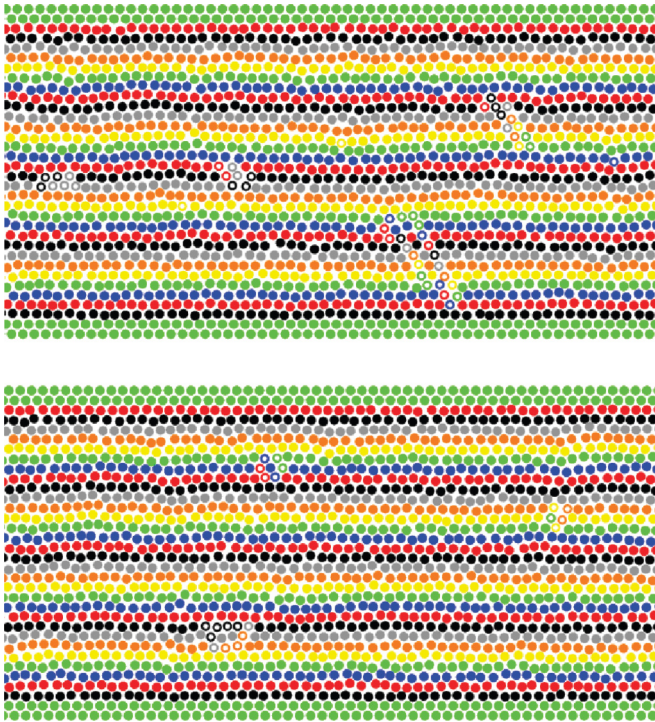
FIG. 13. (Color online) Snapshots of differently sized clusters of particles which moved away from their initial positions. A section of the system is shown, where, at time zero, the subsequent mobile rows are marked by different colors in the y direction (row 1 is black, row 2 is red, row 3 is blue, etc., from bottom to top) to indicate the particles that have left their row at a later time. The whole system consisted of $N = 73\,440$ particles (including walls). Simulations were carried out at $\Delta = 0$, $T = 1$ and with 30 rows. These snapshots were taken at an MD time of 4000 (relative to starting the simulation with the unequilibrated ideal crystalline configuration). Those particles, which are no longer in their initial position, are displayed as circles, all of the other particles as dots.
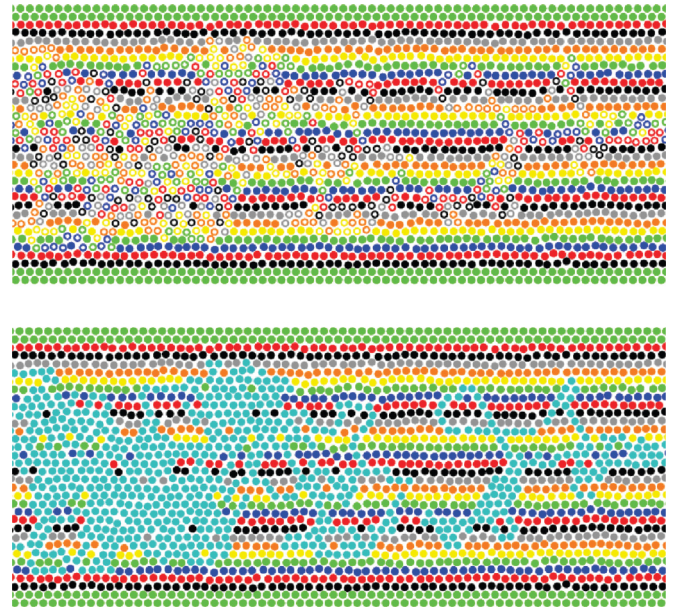

FIG. 14. (Color online) Snapshots showing the results of the "normal" diffusion process. Those particles, which are no longer in their initial position, are displayed as circles, all of the other particles as dots in the upper snapshot. Coloring scheme as described in the caption to Fig. 13. Lower snapshot shows the same section of the system, but displaced particles are shown in blue here, so the crystalline structure, which is still clearly present in the system, becomes more obvious. The whole system consisted of $N = 73\,440$ particles (including walls), $\Delta = 0$, $T = 1$ and 30 crystalline rows.

other by being a high-pressure spot and a low-pressure spot in the crystalline structure, within the resulting recombination times up to several thousand particles can be removed from their initial lattice site.

One snapshot showing the beginning of this "hole and interstitial" diffusion process is given in Fig. 15. One can see the hole at the end on the right-hand side of the wavy line of particles that have been displaced from their initial lattice sites as well as the fact that there is one extra particle for the crystalline structure at the left-hand side inside the "blob" of displaced particles. This is illustrated in the enlarged sections showing that the number of nearest-neighbor particles is not equal to six for all particles around the vacancy and the interstitial: In the proximity of the vacancy we found one particle with eight neighbors and two with seven; in the region with the interstitial two particles have five neighbors and two have seven. The lower graph shows the same section of the system at a later time: Here, the recombination of hole and interstitial has occurred quite soon, leaving behind a closed curve of particles that have been displaced from their initial lattice sites but are sitting in correct (but different) lattice sites again. The creation of these vacancy-interstitial pairs at $T \leqslant 1.0$ are still such rare events that the interaction between

two different pairs is still negligible. But in the case of the smaller rings of particles that have been displaced from their initial lattice sites by jumping into their neighbor's position, the mechanism seems to differ: We observe the process referred to as "cooperative ring rotation process" in Ref. [54].

In the beginning of the research on diffusion in the 1930s and 1940s, different diffusion mechanisms were discussed [55,56] and the idea of diffusion being carried out by groups of particles making cooperative rotations and even direct exchange between two particles was very popular. However, the Kirkendall experiment [57] showed that in metallic alloys the prevalent diffusion mechanism is via vacancies and/or interstitials. Since there has been no experimental evidence for different diffusion mechanisms, the general belief is that cooperative rotation processes play no important role (or do not even exist) in diffusion processes in three-dimensional crystals [54,58,59]. In two-dimensional crystals like the one we are studying here, there are only two other studies describing such cooperative rotations [45,46]. In both of these studies, by Montalenti *et al.*, this particular diffusion mechanism has been found to be extremely rare and could only be observed by applying the rare event sampling technique of temperature-accelerated dynamics (TAD) [43,44]. Of course, they were investigating more complex (and realistic) systems than the one we are studying here, but, still, it is fascinating that such cooperative rotation phenomena can also be observed in our simulations. Due to the less complex model system we used, we were even able to use system sizes and time scales on which many of these rotations occurred, which
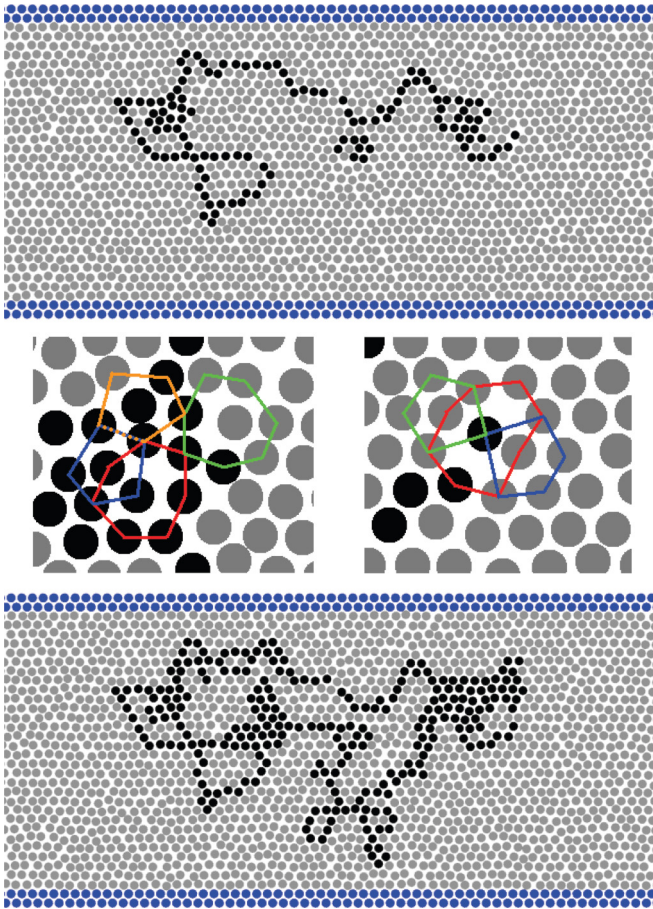
FIG. 15. (Color online) Snapshots illustrating the effect of "normal" diffusion in a simulation at $\Delta = 0$, $T = 1$, 30 rows. A section of the system is shown at two different time steps showing how such a diffusion builds up. Displaced particles are shown as black dots here, while all other particles are shown in grey). The enlarged sections in the middle panel indicate the nearest neighbor particles of those particles which have more or less than six neighbours due to the interstitial particle (left) resp. due to the vacancy (right snapshot), cf. text.

allowed us to gather statistics of the number of particles involved in them and to compare them to the "normal" diffusion phenomena. Investigating these cooperative rotations in detail shows that there is not one distinct particle which starts the movement by being displaced from its original position and leaving behind a hole but that it is a joint movement of the whole group of particles which is induced by thermal fluctuations. While making this concerted rotation movement, some disorder is visible in the crystal around the ring of particles, until the ring has fully turned into its final position and all particles are sitting in lattice sites again. Figure 16 illustrates this process: Initially, there seem to be larger-than-average fluctuations in the area of the crystal left of the ring. Note that there is no real hole or interstitial particle, there is exactly the right number of particles for this part of the crystal (they are only fluctuating strongly). This might "infect" the left particles of the ring, motivating them to fluctuate with a larger amplitude than on average and passing their momentum on to the other particles in the ring. The ring then jointly begins to turn around. In the third snapshot, one can see how the local
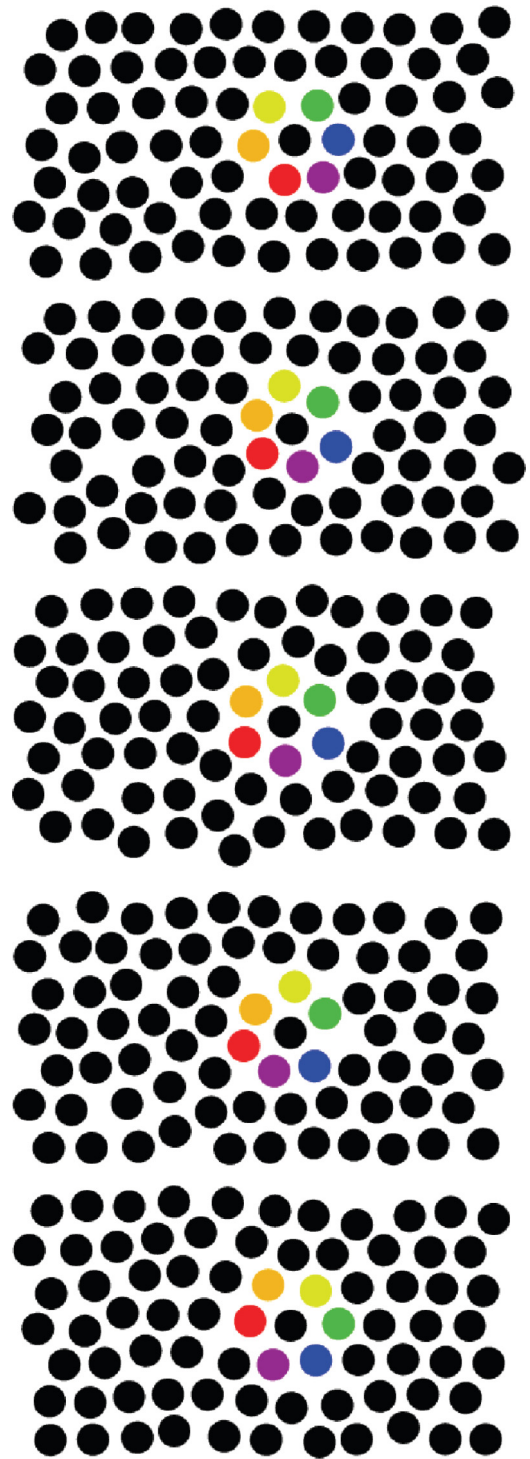

FIG. 16. (Color online) Cooperative ring rotation process shown in a series of snapshots which differ by an MD time difference of 0.4. Simulation at $T = 1$, $\Delta = 0$ and with 30 rows.

structure around the ring has adapted to it: The ring of particles does not fit into the general crystalline structure any more as it has a different angle (relative to the lattice directions at the start of the ring rotation process), but the particles around the ring have adjusted themselves to the ring and not to the rest of the crystal. Finally, the crystalline structure is restored again (which is, after all, energetically preferable) while the particles
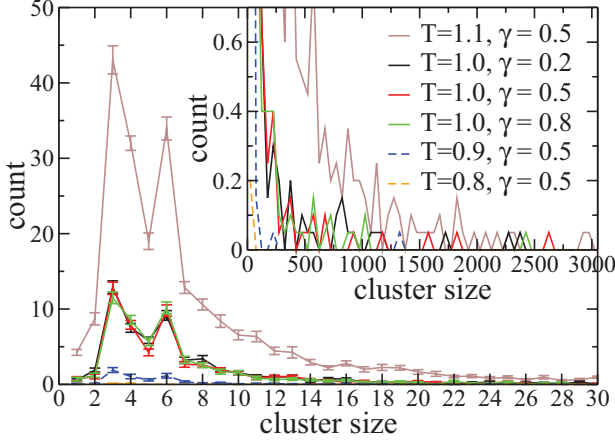
FIG. 17. (Color online) Histograms of the distribution of cluster sizes at indicated temperatures. As expected, the curves are independent of γ (in the range of their errors). (Inset) The distribution of larger clusters; please note that the binning of the histogram is wider there. The data were taken after the simulation had run for 2×10^6 steps; system size was $N = 73\,442$ particles (including walls) and it was averaged over 20 runs.

in the ring turn around further, ending in a position which is commensurate with the crystalline lattice, and the movement stops. These snapshots were taken at intervals of about 200 MD steps, with $\Delta t = 0.002$, so the series of snapshots shown in Fig. 16 covers an "MD time" of $4 \times 0.4 = 1.6$ (with $\gamma = 0.5$ and at $T = 1.0$).

In order to quantify these diffusion phenomena, we recorded histograms showing which cluster sizes occur at which temperature (Fig. 17). We also show in the same graph that the curves are independent of the friction coefficient γ as expected. The clusters with sizes between 2 and about 25 particles correspond to situations where particles have actually swapped positions. In the case of only 2 particles, which is rare, these particles have probably swapped positions during a large fluctuation while all of the other particles that took part in this fluctuation have returned to their initial positions. From three particles onwards, mostly cooperative circular movements have occurred. Cluster sizes of 3 and 6 particles seem to be favored due to the hexagonal lattice structure. Larger clusters correspond to cases where a hole and an interstitial have been created and led to diffusion.

Particles were counted as being displaced if they moved more than half of the average next-neighbor distance away from their initial position. In order to exclude pure fluctuations of particles which moved back into their original position eventually, displaced particles were identified in two snapshots, 10 000 MD steps apart from each other, and only those particles which were displaced in both snapshots were counted here. Ten thousand MD steps was judged to be a suitable time interval here, as single particles easily fluctuate back into their old position on this time scale, but those which have swapped positions practically never go back into their old positions.

Using the values given in Fig. 17, it is possible to estimate the activation energy for ring rotation processes. Fitting the number of occurrence of rings consisting of three particles versus temperature with the formula $y = y_0 e^{-A/T}$,

$k_B = 1$, yields an activation energy of $A \approx 13.8$. Fitting the corresponding curve of the number of occurences of rings consisting of six particles yields a slightly higher activation energy of $A \approx 14.1$, which is not surprising as larger rings are clearly more difficult to rotate. Of course, these values are only a rough estimate as we had merely four different temperatures to base the fit on.

In order to estimate the contribution of the cooperative ring rotation processes to the diffusion constant, one can show that each particle which is not in its initial position any more, but instead sits in one of its neighbors' lattice site, contributes $\frac{1}{N}a^2$ to the MSD, a being the crystal's lattice constant:

If $M_s(t) = \frac{1}{N}\sum_{i=1}^{N}[x_i(t) - x_i(0)]^2$ denotes the MSD with respect to the starting configuration, let $M_{s,0}(t)$ denote the MSD of such particles which do not participate in any rotation processes (and, for simplification, also not in any other diffusion process). Let us assume that this $M_{s,0}(t) = c_0$ for all times t greater than a small time t_s in which a harmonic movement of the particles is visible [i.e., if one would plot $M_{s,0}(t)$ one would see an overshoot for very small times t and then just a straight horizontal line].

We then can calculate the MSD $M_{s,1}(t)$ of *only* particles which do participate in a ring rotation process and each of which move onto a neighbor's lattice site in this process; thus, they all move exactly one lattice constant a away from their initial lattice site and then fluctuate around this new lattice site. For this $M_{s,1}(t)$ of the N_0 particles which participate in this rotation we can write

$$M_{s,1}(t) = \frac{1}{N_0}\sum_{i=1}^{N_0}[x_i(t) - x_i(0)]^2$$
$$= \frac{1}{N_0}\sum_{i=1}^{N_0}[x_i(t) - x_i(T_0) + x_i(T_0) - x_i(0)]^2 \quad (3)$$

with T_0 denoting a time where the particles have just moved onto the new lattice sites, yielding $x_i(T_0) - x_i(0) = a$ and $x_i(t) - x_i(T_0)$ being the distance between a particle and its new lattice position which is for $t - T_0 \gg t_s$ *on average* the distance which the nonrotated particles have from their (initial) lattice positions as well. Thus,

$$\frac{1}{N_0}\sum_{i=1}^{N_0}[x_i(t) - x_i(T_0)]^2$$
$$= \frac{1}{N_0}\sum_{i=1}^{N_0}\left[x_i^2(t) - 2x_i(t)x_i(T_0) + x_i^2(T_0)\right] = m_0(t) = c_0.$$
$$(4)$$

Therefore, we can write Eq. (3) as

$$M_{s,1}(t) = M_{s,0}(t) + 2a\frac{1}{N_0}\sum_{i=1}^{N_0}[x_i(t) - x_i(T_0)] + a^2$$
$$= M_{s,0}(t) + a^2 \quad (5)$$

as $\frac{1}{N_0}\sum_{i=1}^{N_0}[x_i(t) - x_i(T_0)] = 0$ if we average over enough particles, as some particles move to the right-hand side and some to the left [always measuring distances from their new lattice site $x_i(T_0)$], and, thus, the average should be zero.
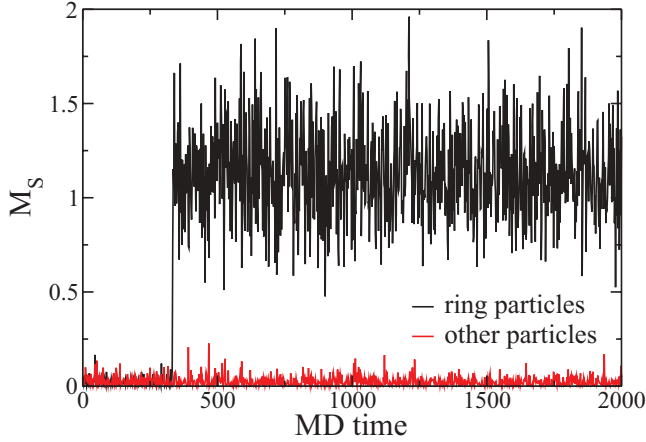
FIG. 18. (Color online) Contribution of a cooperative ring rotation process to the M_s: Just as calculations show, the MSD of those particles which participated in the rotation process (referred to as "ring particles" in the legend) is (on average) increased by a^2, a being the lattice constant, in comparison to the MSD of particles which did not participate in the rotation process ("other particles"). Simulation at $T = 1$, without misfit. System size was $N = 73\,440$ particles (including walls).

Thus, the MSD of the whole system composed of N particles out of which N_0 participate in a rotation movement reads

$$M_s(t) = \frac{1}{N}[(N - N_0)M_{s,0}(t) + N_0(M_{s,0}(t) + a^2)]$$
$$= M_{s,0}(t) + \frac{N_0}{N}a^2. \qquad (6)$$

This can easily be checked through simulations, shown in Fig. 18: The difference between the averaged MSD before the particles have made a circular movement is (within the small errors) smaller than after the circular movement exactly by a^2, when each particle sits on its neighbors' lattice site. The fluctuations are larger, though, as the MSD is calculated with respect to the "old" lattice site.

In order to get an idea about the size of the contribution of the circular movements to the MSD (and, therefore, to the diffusion constant), one can have a look at Fig. 17 again: It shows that in a typical run at $T = 1.0$ after 2 million steps there are about 400 particles which are displaced from their initial lattice sites through circular movements, but about a few thousand which are displaced due to the "normal" diffusion mechanism of hole and interstitial. Therefore, the "normal" diffusion mechanism contributes considerably more to the MSD. Actually, the contribution of a single event, where, for example, a ring of 6 particles makes a circular movement, cannot be seen in the MSD at all, as its contribution is just $6\frac{1}{N}a^2$, which is smaller than the fluctuations of the MSD, at least for the large system with 64 800 mobile particles. So the steep parts of the MSD shown in Fig. 12 are due to the "normal" diffusion processes, which involve a few hundred or even a few thousand particles and not due to such small circular movements. The small circular movements are, therefore, not visible in this plot. At slightly lower temperatures, however, such large-scale diffusion processes seem to vanish (compare

Fig. 17). Unfortunately, also circular movements become much rarer in this case.

In order to quantify the diffusion, we calculated the diffusion constant C_D by fitting the MSD (which we obtained from averaging over 20 simulation runs at temperatures $T = 0.9$, 1.0, and 1.1) with the formula $M_s = y_0 + 6C_Dt$. The offset y_0 was necessary, because we started out with equilibrated configurations. This yielded the following values of the diffusion constant:

T	0.9	1.0	1.1
C_D	1.90×10^{-6}	5.72×10^{-6}	3.05×10^{-5}

Fitting these values via $C_D = C_{D,0}e^{-A/T}$, $k_B = 1$, in order to obtain an estimate for the activation energy of the diffusion, yields $A \approx 17.7$, which is higher than for the rings consisting of three or six particles. Again, this is not surprising as the formation of a hole and an interstitial introduces more disorder into the crystal than a rotation of some particles. This also indicates that ring rotations are to be expected to occur at slightly lower temperatures than diffusion mechanisms based on holes and interstitials. And even if the circular movements do not play an important role for the overall diffusion constant in this particular system, they might do so in other systems where the range of temperatures where ring rotations do already occur, but holes are not yet created, might be larger than here.

The MD time scale of the circular movements of small groups of particles is between 0.4 and 2.5, i.e., with $\Delta t = 0.002$ they needed about 200–1200 MD steps. Figure 19 gives a rough idea of the time scale of the cooperative ring rotations and its distribution. Larger clusters seem to need more time. For comparison: A cluster which was built up by "normal" diffusion processes (but was comparably small for such a cluster) consisting of 58 displaced particles needed an MD time of 4.8. Larger rings of particles seem to need more time (see Fig. 19).
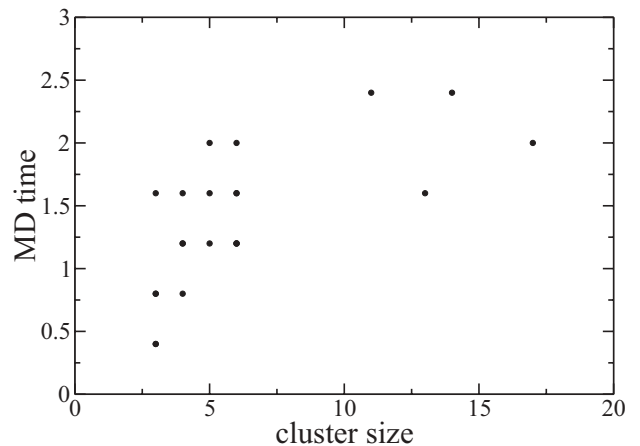

FIG. 19. MD time which the cooperative ring rotation needed versus cluster size. MD time is only computed down to an accuracy of 0.4 as this already meant that snapshots had to be written out after every 50 steps. System size $N = 73\,442$ particles, $T = 1$, no misfit. These data points are only meant to give a rough idea of the time scale of the cooperative ring rotations.

The larger "normal" diffusion processes including a pair of a hole and an interstitial need generally more time but usually also affect many more particles. Their time scale depends strongly on the cluster size. For example, a very small such cluster composed of 58 particles needed an MD time of 4.8, while clusters composed of some 1000 particles can easily need around 1×10^6 steps, i.e., an MD time of $1 \times 10^6 \times 0.002 = 2000$. It varies very strongly, of course, as sometimes holes and interstitial particles recombine very quickly and sometimes they do not. Typical time scales of these processes can be read off from Fig. 12 as the "steps" in the MSD correspond to these "normal" diffusion processes, building up large clusters of displaced particles.

V. CONCLUDING REMARKS

To conclude, we have conducted a thorough study of the different types of motion in two-dimensional colloidal crystals confined between walls that were composed of rigid particles and that were placed at commensurate or incommensurate distances. We have observed motion on different length and time scales: In the case with commensurate walls, where the crystal is not compressed, the MSD of the particles is finite in the x direction as well as in the y direction, as the walls pin the particles and prevent any movement of the center of mass. The MSD is larger for rows inside of the crystal than for rows close to the walls as the walls impose a boundary condition of zero amplitude for the phonons.

If the walls are placed closer together, thus compressing the crystal, the MSD of the particles becomes smaller as there is less space available per particle. The MSD shows no sign of the proximity of the structural transition, which occurs when the walls are placed even closer together and one of the crystalline rows disappears, which leads to the creation of solitons.

Once this structural transition has taken place, the MSD changes significantly: Now the MSD still has the smallest values for the rows directly adjacent to the walls but has the largest values for the rows directly next to the rows adjacent to the walls, as the solitons are located there. Further inside the crystal, the MSD decreases (instead of increasing) but is still considerably larger than in the case without solitons. Additionally, due to the incommensurability of the number of particles per row, the inner rows are no longer pinned by the potential created by the walls and the center of mass is free to move. Therefore, the MSDs of all rows except the rows directly adjacent to the walls do not reach a plateau at all any more. This structural transition needs considerably more MD time than the average equilibration time in this system.

The MSD of the solitons differs significantly from the MSD of the particles. It is almost negligible in the y direction, but an order of magnitude larger than the MSD of the particles in the x direction, as the center of the solitons can already move by a few interparticle distances if the particles involved in it only make a small coordinated movement in one direction. As the solitons are arranged in a lattice similar to a crystal and interact with each other via a harmonic potential as previous work has shown [27], their mean-square displacements also show an initial overshoot. As the "spring constant" mediating the interaction of the solitons is small, this overshoot can be seen at time differences which are again an order of magnitude larger than in the case of the mean-square displacement of the particles.

We have also presented results on the diffusion processes occurring in colloidal crystals. In addition to the well-known diffusion mechanism in which a pair of a hole and an interstitial is created, diffuses, and, finally, annihilates itself again, we have found that, in this particular system, cooperative ring rotation processes are common. They can involve different numbers of particles, but three or six particles are the preferred numbers due to the hexagonal lattice structure, and the diffusion occurs by a concerted and simultaneous movement of all of these particles, which move into their neighbor's lattice site. These rotation processes do not contribute to overall diffusion as much as the hole-and-interstitial processes, but that is only due to the much smaller number of particles involved in these ring rotation processes. They do, however, occur much more frequently than the hole-and-interstitial processes. Including hydrodynamic interactions into the simulations might even enhance the rate at which ring rotations occur. It is especially remarkable that these effects occurred so very frequently in our system, as in other simulations such ring rotation events have been observed only very rarely. For instance, the study described in Ref. [45] had to be carried out using temperature-accelerated dynamics, which is a kind of rare event sampling, while in the system and at the temperatures that we studied, these events were not rare at all. Of course, this is probably due to the fact that our model is much simpler. Still, we feel that these cooperative ring rotations should not be neglected when diffusion in two-dimensional crystals and at interfaces is studied, as it is possible that they play an even more important role in other systems.

[1] W. C. Poon and P. N. Pusey, in *Observation, Prediction and Simulation of Phase Transitions in Complex Fluids*, edited by M. Baus (Kluwer, Dordrecht, 1995), p. 3.

[2] H. N. W. Lekkerkerker, in *Observation, Prediction and Simulation of Phase Transitions in Complex Fluids*, edited by M. Baus (Kluwer, Dordrecht, 1995), p. 53.

[3] T. Palberg, Curr. Opin. Colloid Interface Sci. **2**, 607 (1997).

[4] H. Löwen, J. Phys.: Condens. Matter **13**, R415 (2001).

[5] H. Löwen and C. N. Likos (eds.), *Colloidal Dispersions in External Fields*, Special Issue of J. Phys.: Condens. Matter **16**, 38 (2004).

[6] K. Zahn, J. M. Mendez-Alcaraz, and G. Maret, Phys. Rev. Lett. **79**, 175 (1997).

[7] Q. H. Wei, C. Bechinger, D. Rudhardt, and P. Leiderer, Phys. Rev. Lett. **81**, 2606 (1998).

[8] K. Zahn, R. Lenke, and G. Maret, Phys. Rev. Lett. **82**, 2721 (1999).

[9] K. Zahn and G. Maret, Phys. Rev. Lett. **85**, 3656 (2000).

[10] C. Eisenmann, P. Keim, U. Gasser, and G. Maret, J. Phys.: Condens. Matter **16**, S4095 (2004).

[11] K. Zahn, A. Wille, G. Maret, S. Sengupta, and P. Nielaba, Phys. Rev. Lett. **90**, 155506 (2003).

[12] H. König, R. Hund, K. Zahn, and G. Maret, Eur. Phys. J. E **18**, 287 (2005).

[13] M. Koppl, P. Henseler, A. Erbe, P. Nielaba, and P. Leiderer, Phys. Rev. Lett. **97**, 208302 (2006).

[14] L. Assoud, F. Ebert, P. Keim, R. Messina, G. Maret, and H. Löwen, J. Phys.: Condens. Matter **21**, 464114 (2009).

[15] F. Ebert, P. Dillmann, G. Maret, and P. Keim, Rev. Sci. Instrum. **80**, 083902 (2009).

[16] F. Ebert, G. Maret, and P. Keim, Eur. Phys. J. E **29**, 311 (2009).

[17] P. Henseler, A. Erbe, M. Koppl, P. Leiderer, and P. Nielaba, Phys. Rev. E **81**, 041402 (2010).

[18] A. Chowdhury, B. J. Ackerson, and N. A. Clark, Phys. Rev. Lett. **55**, 833 (1985).

[19] K. Franzrahe, P. Nielaba, A. Ricci, K. Binder, S. Sengupta, P. Keim, and G. Maret, J. Phys.: Condens. Matter **20**, 404218 (2008).

[20] T. Bohlein, J. Mikhael, and C. Bechinger, Nat. Mater. **11**, 126 (2012).

[21] D. M. Herlach, I. Klassen, P. Wette, and D. Holland-Moritz, J. Phys.: Condens. Matter **22**, 153101 (2010).

[22] S. Medina, P. Virnau, and K. Binder, J. Phys.: Condens. Matter **23**, 035105 (2011).

[23] J. J. Crassous, M. Siebenbürger, M. Ballauff, M. Drechsler, D. Hajnal, O. Henrich, and M. Fuchs, J. Chem. Phys. **128**, 204902 (2008).

[24] R. Haghgooie and P. S. Doyle, Phys. Rev. E **72**, 011405 (2005).

[25] Y. H. Chui, S. Sengupta, and K. Binder, Europhys. Lett. **83**, 58004 (2008).

[26] Y. H. Chui, S. Sengupta, I. K. Snook, and K. Binder, J. Chem. Phys. **132**, 074701 (2010).

[27] Y. H. Chui, S. Sengupta, I. K. Snook, and K. Binder, Phys. Rev. E **81**, 020403(R) (2010).

[28] D. Wilms, N. B. Wilding, and K. Binder, Phys. Rev. E **85**, 056703 (2012).

[29] P. M. Chaikin and T. C. Lubensky, *Principles of Condensed Matter Physics* (Cambridge University Press, Cambridge, UK, 1995).

[30] M. Leitner, B. Sepiol, L.-M. Stadler, B. Pfau, and G. Vogl, Nat. Mater. **8**, 717 (2009).

[31] F. Faupel and K. Rätzke, in *Diffusion in Condensed Matter*, edited by P. Heitjans and J. Kärger (Springer, Berlin, 2005), p. 267.

[32] M. L. Grant, B. S. Swartzentruber, N. C. Bartelt, and J. B. Hannon, Phys. Rev. Lett. **86**, 4588 (2001).

[33] R. van Gastel, E. Somfai, S. B. van Albada, W. van Saarloos, and J. W. M. Frenken, Phys. Rev. Lett. **86**, 1562 (2001).

[34] P. J. Feibelman, Phys. Rev. Lett. **65**, 729 (1990).

[35] Z.-P. Shi, Z. Zhang, A. K. Swan, and J. F. Wendelken, Phys. Rev. Lett. **76**, 4927 (1996).

[36] T. R. Linderoth, S. Horch, L. Petersen, S. Helveg, E. Laegsgaard, I. Stensgaard, and F. Besenbacher, Phys. Rev. Lett. **82**, 1494 (1999).

[37] F. Montalenti and R. Ferrando, Phys. Rev. Lett. **82**, 1498 (1999).

[38] J. M. Cohen, Surf. Sci. Lett. **306**, L545 (1994).

[39] T. Ala-Nissila, R. Ferrando, and S. C. Ying, Adv. Phys. **51**, 949 (2002).

[40] K. F. McCarty, J. A. Nobel, and N. C. Bartelt, Nature **412**, 622 (2001).

[41] Z. Wang, F. Wang, Y. Peng, Z. Zheng, and Y. Han, Science **338**, 87 (2012).

[42] X.-M. Bai and M. Li, Phys. Rev. B **77**, 134109 (2008).

[43] M. R. Sorensen and A. F. Voter, J. Chem. Phys. **112**, 9599 (2000).

[44] F. Montalenti and A. F. Voter, J. Chem. Phys. **116**, 4819 (2002).

[45] F. Montalenti, A. F. Voter, and R. Ferrando, Phys. Rev. B **66**, 205404 (2002).

[46] M. R. Sorensen, Y. Mishin, and A. F. Voter, Phys. Rev. B **62**, 3658 (2000).

[47] I. K. Snook, *The Langevin and Generalized Langevin Approach to the Dynamics of Atomic, Polymeric and Colloidal Systems* (Elsevier, Amsterdam, 2007).

[48] HOOMD-BLUE Web page http://codeblue.umich.edu/hoomd-blue.

[49] J. A. Anderson, C. D. Lorenz, and A. Travesset, J. Comput. Phys. **227**, 5342 (2008).

[50] M. P. Allen and D. J. Tildesley, *Computer Simulation of Liquids* (Oxford University Press, Oxford, UK, 1989).

[51] D. J. Evans and G. P. Morriss, *Statistical Mechanics of Nonequilibrium Liquids*, 2nd ed. (Cambridge University Press, Cambridge, UK, 2008).

[52] K. Bagchi, H. C. Andersen, and W. Swope, Phys. Rev. E **53**, 3794 (1996).

[53] D. R. Nelson, in *Phase Transitions and Critical Phenomena*, edited by C. Domb and J. L. Lebowitz, Vol. 7 (Academic, London, 1983), p. 1.

[54] G. E. Murch, in *Phase Transformations in Materials*, edited by G. Kostorz (Wiley VCH, Weinheim, 2001), p. 192.

[55] C. Zener, Acta Crystallogr. **3**, 346 (1950).

[56] A. S. Nowick, Annu. Rev. Mater. Sci. **26**, 1 (1996).

[57] A. D. Smigelskas and E. O. Kirkendall, Trans. AIME **171**, 130 (1947).

[58] D. Lazarus, in *Diffusion in Crystalline Solids*, edited by G. E. Murch and A. S. Nowick (Academic Press, Orlando, FL, 1984), p. xii.

[59] W. Frank, U. Gösele, and H. Mehrer, in *Diffusion in Crystalline Solids*, edited by G. E. Murch and A. S. Nowick (Academic Press, Orlando, FL, 1984), p. 66.